Molecular Structure of Charge Control Agents (CCA) and Toner Triboelectrification II: The Role of a Molecular Region with the Same Polarity as CCA Charging in Toner Triboelectrification Phenomena

Norie Matsui

Corporate Research Laboratory, Fuji Xerox Co., Ltd., Kanagawa, Japan

A novel model related to triboelectric charging phenomena in toners containing charge control agents (CCA), used as marking materials in copy machines in electrophotography, is proposed. The model was evaluated by comparing the results from computer chemistry using the molecular orbital method (MO), molecular mechanics method (MM), and Monte Carlo method (MC), with the results from measuring triboelectric charge of several toners containing various CCA. The model is based on the interaction of water molecules and CCA molecules. The CCA is divided into two reciprocal polarity regions in the molecule; one region with the same polarity as the CCA charge and another region with the contrary polarity to the CCA charge. The two regions play different roles in CCA toner charging phenomena. Therefore, the polarity and magnitude of the charging is determined from balancing the intensity of interactions among the each region in the CCA molecule and the water molecule. The consequence of molecule structure of CCA to toner charging is elucidated.

Introduction

The control of both the polarity and magnitude of triboelectric charging is highly significant in toners as an electrophotographic developer. Numerous materials as charge control agents (CCA) are often added to toner particles to control the both triboelectric properties. The problem of triboelectric charging on the toners containing the CCA (CCA toner) has been investigated for a number of years by various authors from different points of view. Their reports mentioned about the charging control ingredient of developer for electrophotography have been roughly divided between two types of mechanisms: electronic transfer[1–3] and ionic transfer.[4–7] The driving force of both transfer types is the electrochemical potential difference. The triboelectric charging continues up to no difference. In the other model for CCA toner charging, its carrier alternates ions and electrons according to the conditions, e.g., materials and atmosphere.[8] These investigations were limited only to restrictive kind of materials. Furthermore, no one has been able to predict the triboelectric charge based on the results of calculations or of the physical properties except for empirical parameters. They only interpret the triboelectric charging phenomenon.

On the other hand, toner concentration (C_t) or CCA concentration (C_A) has been studied as significant factors which control the magnitude in order to optimize electrophotographic parameter.[9–13] They showed that the

magnitude depends on the C_t or the C_A, when all the other factors are constant. Besides, they also showed that the magnitude is influenced by the charge exchange electric field (E_e). The E_e is created during the contact of carrier beads with toner particles, and derives from integrant materials in the carrier or the toner. They, however, didn't elucidate the origin of E_e and the participation of molecular structure and E_e. But it is also important for many material researchers and developers who intend to control the triboelectric charging polarity and magnitude using new materials, to elucidate the relation between molecular structure of materials and the properties of charging than to do the C_t and the C_A.

A toner charging model, the *Water Dissociation Model* (WDM) excellently predicted the triboelectric charge from the results of calculations using only atomic properties.[14,15] The model was also elucidated, systematically and quantitatively comparing the results of computer chemistry based on the model with the observed triboelectric charge of some CCA toners containing various kinds of CCA. The model explains the role of the region with a polarity opposite to the CCA charging polarity in the CCA toner triboelectrification phenomenon. The region was adjudged to be the catalyst in the dissociation of water molecule around the CCA into ions, OH^- and H^+ or H_3O^+. This model also consists with many investigators' experiences, such as the existence and quantity of water has a great influence on the triboelectric charging phenomena.

In this article, a new model, the *Ion Retransfer Model*[16] (IRM), is evaluated as one of a pair of charging mechanisms. This is mutually supplementary to the previous model, the WDM. These two models can systematically explain the role that the molecular structure of the CCA

plays in triboelectric charging in a normal atmosphere. We suggest that the charging magnitude and polarity result from a balance between the interaction of water and the two regions of the CCA molecule with opposite polarities, respectively. Thus we will investigate the model, simulating the triboelectric charging phenomenon based on IRM and measuring the triboelectric charge magnitude on CCA toners.

Charging Model

Both the charging models, the WDM[14,15] and the IRM,[16] are described here.

The CCA which make toner particles charge rapidly and sufficiently, the excellent CCA, have similar steric structure and electrical distribution among all the molecular structures. For example, an excellent negative CCA toner, which can rapidly charge up to required negative charge as a developer used in electrophotography, is composed of a region with a localized positive charge on its surface and a region with a delocalized negative charge on its surface. In most cases of typical excellent negative CCA, the region of localized positive charge is the cation, and the region of delocalized negative charge is the anion. Furthermore the extent of the localization depends on the size of the cation. If the cation is small, i.e., a metal ion, the localized positive charge is the cation itself. If the cation is large, there is a particular region with convergent positive charge on cation surface. In contrast, every anion in the CCA has a characteristically large size and very dilute negative charges uniformly distributed over its entire surface. By then, in the case of a typical excellent positive CCA, the characteristics of its steric structure and charge distribution are wholly counter to those of the previous negative charging CCA. Such CCA contains one region or anion with a concentrated negative charge and the other region or cation with very dilute positive charges uniformly distributed over its surface. Thus it is found that the characteristic steric structure and charge distribution of the CCA have a significant effect on the toner-charging phenomenon. This effect could be explained by both models, WDM and IRM.

Initially, we simply describe the WDM. Although the model has been described in a previous report,[14,15] the description is necessary for understanding the IRM better. The WDM shows that the region with polarity counter to the CCA toner charging contributes to the triboelectric charging phenomenon. In a salt structure compound the region is an ion, or a non-salt CCA molecule has a charge-localizing region. Initially in the model, it was presupposed that the CCA molecule contained in the CCA toner particle exists on its surface.[14,15] This presupposition is considered to be accurate for the actual CCA toner particle surface. Generally, when a low molecular weight compound is added to a resin, the compound migrates from the bulk to the surface, as is well known. Because the usual toner particles are manufactured by pulverizing after melt-mixing the ingredients, the parts of aggregated low molecular weight compound are more easily pulverized than the other parts, so that CCA molecules are readily exposed on the toner particle surface. The molecule has previously adsorbed many water molecules from the atmosphere before the toner particle contacts with a carrier bead to produce triboelectric charge as a developer for electrophotography. At the time of the contact, a *water bridge* between the CCA molecule and the carrier bead is instantly constructed by hydrogen bonding (Fig. 1). The
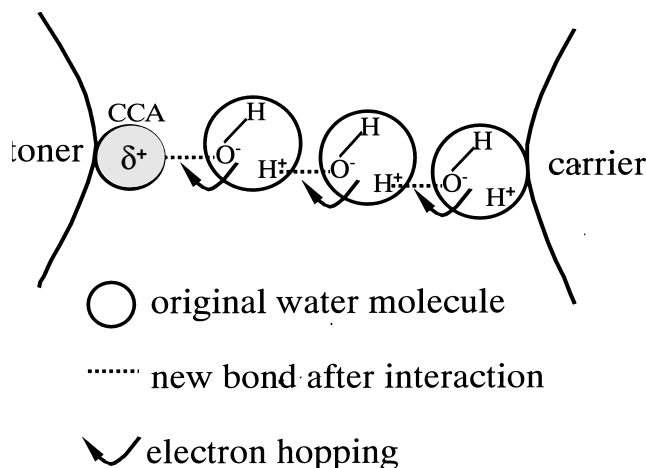

Figure 1. Diagram of *water bridge* and of negative toner's triboelectric charging phenomenon containing negative CCA.

terminal water molecule on the CCA side of the *water bridge* is then polarized, under the effect of the region of the CCA whose charge polarity is counter to the CCA charging polarity, and is concentrated on it. Subsequently the water molecule is dissociated and produces H^+ or H_3O^+ and OH^-, according to the degree of charge convergence and the steric structure of the CCA (Fig. 2). The region with the more negative and concentrated charge than the other region of the CCA molecule attracts the proton of the water molecule, and the polarization between hydrogen and oxygen in water molecule is induced, if the CCA is used in a positive charging toner (the upper diagram in Fig. 2). In contrast, if the CCA is used in a negative charging toner, the concentrated positive charge region attracts the oxygen atom of the water molecule, because the oxygen atom polarizes more negatively than hydrogen in a water molecule (the lower diagram in Fig. 2). Thus the orientation of the terminal water molecule of the *water bridge* toward the CCA molecule depends on the polarity and the degree of charge convergence on the CCA molecule surface as mentioned above. As a consequence of the polarization and of the interaction among numerous water molecules around the contact point of the CCA with the carrier bead, both terminal water molecules of the *water bridge* are dissociated into OH^- and H^+ or H_3O^+ (Fig. 2). Each ion adheres to the CCA on the toner surface or to the carrier beads, respectively. If the CCA is for a negative charging toner, OH^- is attracted to the concentrated positive part of the CCA molecule; consequently the CCA toner will charge negatively. In the contrary case, when it is a positive CCA, H^+ or H_3O^+ is attracted to concentrated negative part of the CCA molecule and it will charge positively. On the other hand, the triboelectric charging magnitude of the CCA depends on its ability to dissociate water and attract individual dissociated ions, either H^+(or H_3O^+) or OH^-. Therefore, a superior negative CCA molecule based on the model should contain a region with a concentrated and large positive charge on its surface. Concretely, a large size cation in a salt structure compound or one not having a salt structure should contain the region with a concentrated positive charge on its surface. A small cation in the salt structure compound should itself have a large positive charge. In the contrast, a superior positive CCA based
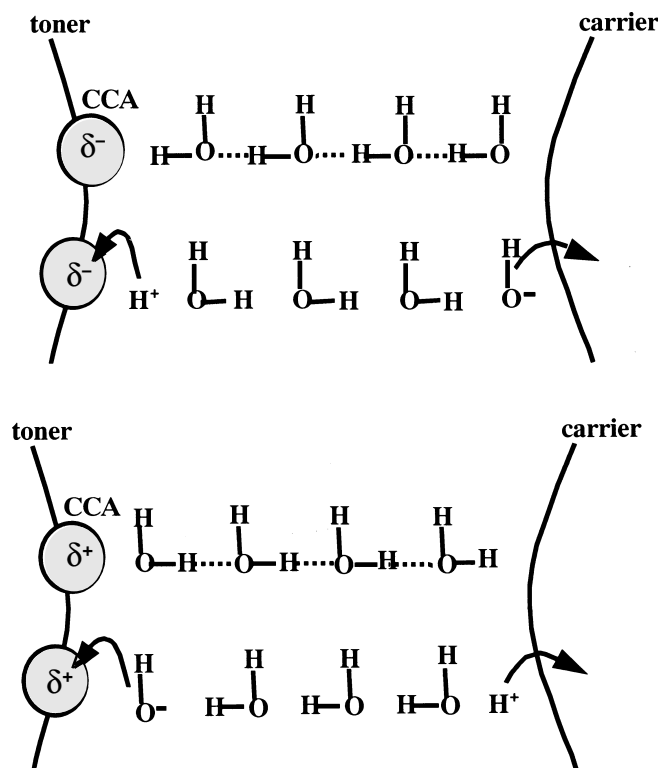
Figure 2. Diagram of the CCA toner charging mechanism through dissociation of both terminal water molecules of *water bridge*. The upper section shows the positive charging phenomenon and the lower section the negative.
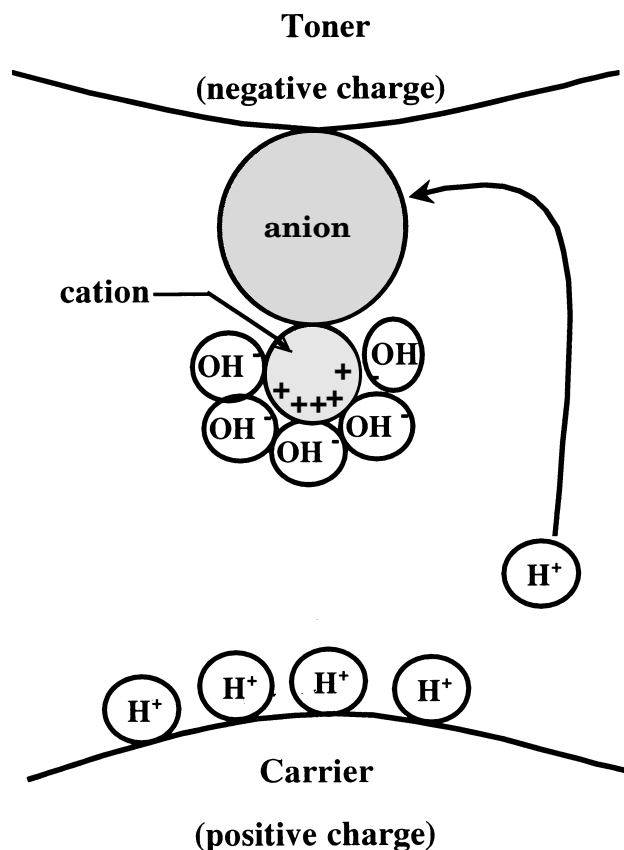

Figure 3. Diagram of mechanism of negative CCA toner's charge decrease due to H^+ re-transferring from carrier bead surface to CCA toner surface.

on the model should contain polarity opposite to the negative CCA, as mentioned above.

The second mechanism is the IRM. The aforementioned model, WDM, elucidates that CCA dissociates water molecule to ions and they transfer to toner surface. But the model does not deal with the movement of ions after transferring. The dissociated ions are very small, thereby they are very mobile. Therefore we propose the second model, IRM. This model treats the role of other regions with the same charge polarity as the CCA. In the region of a typical superior CCA molecule, there is no concentrated charge with the same polarity as the CCA charging on its surface. In most cases of a typical superior negative CCA, its anion size is far greater than the cation size and an extremely small positive charge is uniformly distributed on the anion surface, in contrast to the negative charge converging at the core of a large anion. This structure is explained based on the IRM; the CCA charge is prevented from decreasing (by the counter ion retransferring from the carrier bead surface to the CCA) after CCA charging by attracting the requisite water ion. For example, in the case of a negative CCA, the region with the concentrated positive charge of the CCA attracts OH^- after dissociating the water molecule into two kinds of ions, and the other H^+ or H_3O^+ transfers to the carrier surface by the WDM. At this time, the CCA toner charges negatively. But the contact between the CCA toner particle and the carrier bead is maintained for a long time after the initial contact in triboelectrically charging. Then if the H^+ ions on the carrier bead retransfers to the toner, the negative CCA toner charge decreases according to number of H^+ ions (Fig. 3). In contrast if the OH^- ions re-

transfer to the toner, the total negative charge of toner increases during the contact time (Fig. 4). In this case the anion has an idiosyncratic electrical structure; the anion is greatly polarized: negative charges exist in the center of the anion and positive charge resides on the anion surface, though the net charge of the anion is negative. Thus it appears that the number and kind of retransferring ion depends on the charge distribution on the surface of the region with the same charge polarity as the CCA charging.

Based on both models, a charge structure of the superior CCA should be described as follows. In the case of negative CCA, its molecule should be composed of a region or a small cation with a concentrated positive charge on its surface in order to attract the OH^- ions and another region or a large anion with dilute negative charges distribution on its surface to inhibit H^+ from retransferring, or with a concentrated negative charge in its core and a concentrated positive charge on a narrow region of its surface to attract more OH^- ions (Fig. 4). On the contrary the case of positive CCA should be composed of a region or a small anion with a concentrated negative charge on its surface in order to attract the H^+ and another region or a large cation with a dilute positive charge distribution to inhibit OH^- from retransferring, or with a concentrated positive charge in its core and a concentrated negative charge on a narrow region of its surface to attract more H^+ ions.

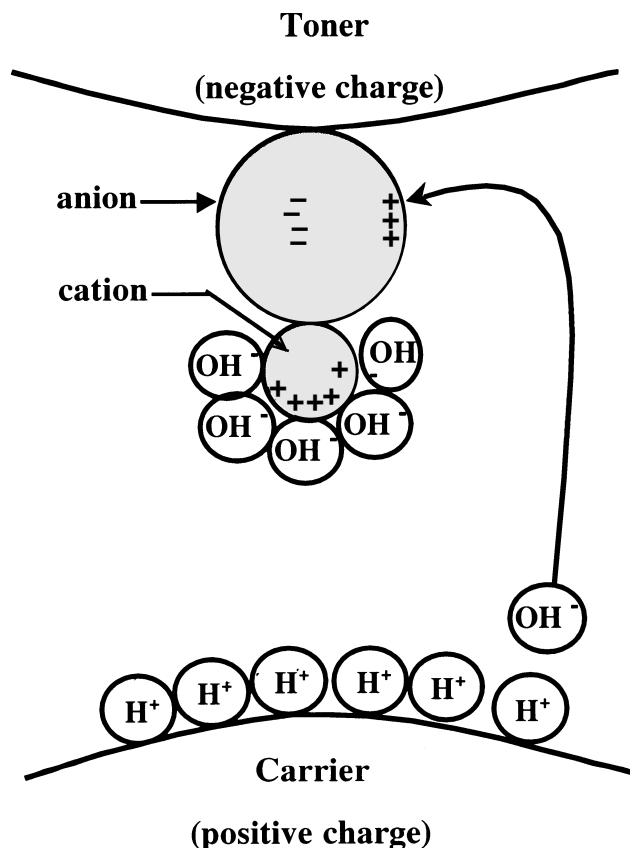We then quantitatively evaluated the models by comparing simulations based on the models with measure-

Toner

(negative charge)

anion →

cation —

Carrier

(positive charge)

Figure 4. Diagram of mechanism of negative CCA toner's charge increases due to OH⁻ approaching CCA toner surface.

Figure 5. Diagram of *Ion Retransfer Model* (IRM) of negative CCA.

ment of the triboelectric charging magnitude on CCA toners.

Experimental

The verification of the WDM has been reported in the previous study.[14,15] In that study, the observed results consisted of results from simulations based on the model. Therefore, in this article we will evaluate only the IRM. We use computer chemistry for the evaluation of the model, because the CCA used in electrophotography has a complicated chemical structure; predicting their abilities to dissociate the water molecules, to attract the dissociated ions, and to charge toner cannot be done simply by viewing its chemical structure drawn on paper. Using the computer chemistry method, we easily observe the accurate steric structure and calculate charge distribution in the CCA molecule and simulate to reduce charge on it.

We will describe in detail the calculation procedure for the negative charging CCA, whose structure is composed of an anion and a cation as a salt. In the first step it was assumed that the cation attracts an OH⁻ ion and subsequently the CCA charges negatively. This process is based on the WDM. On the next step, we simulated the manner in which numerous H⁺ ions approach the complex composed of the CCA molecule and one OH⁻ ion, and the number of H⁺ ions in a specific range from the CCA molecule was regarded as the ability to inhibit the decrease of the CCA charge (Fig. 5). A more concrete procedure is as follows.
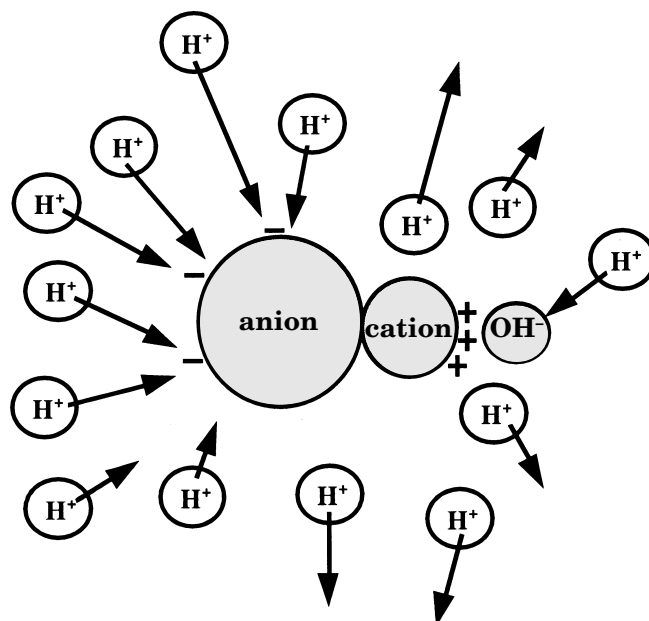
Optimization of CCA Molecules. In the case of a CCA composed of a cation and an anion, at first the ions are distributively optimized and then optimized together as a CCA molecule in a Dreiding force field[17] and charge equilibration method.[18] Insofar as the force field and the charge calculation method do not contain all atoms' parameters, Na⁺ and Fe are substituted for K⁺ and Cr, respectively. The optimized CCA has the most stable steric structure and charge distribution with the lowest energy. In other cases of non-salt structures, the CCA is optimized using the same method as in the former case. For the optimization we use a commercial program, POLYGRAF® version 2.20 (Molecular Simulation Inc.).

Optimization of CCA and OH⁻ Complex. The most stable steric structure and charge distribution on the complex are obtained using the POLYGRAF®, as in the above procedure. The complex is now described as CCA-OH. A semiempirical molecular orbital method, the Modified Neglect of Diatomic Overlap (MNDO)[19] used in the previous study of the WDM was used to optimize a low molecular weight compound as a water molecule or a highly symmetrical molecule as the tetraphenyl borate ion. But it was not suitable for a compound with a very complicated chemical structure such as the CCA in verifying the IRM. However, POLYGRAF® is a very effective tool to optimize the chemical structure of complicated compounds. Because a compound possesses numerous degrees of freedom among atomic combinations, it has numerous metastable, i.e., local minimum states. Thus it is hard to determine the most stable molecule structure with the lowest energy, the global minimum energy. But a molecular dynamics method (MD) in POLYGRAF® can surmount many energy barriers among metastable states by repeating the process of raising temperature up to a point sufficient to surmount an energy barrier, followed by annealing to room temperature, sequentially it can approach more handily to the most stable state corresponding to the global minimum energy than MNDO can.
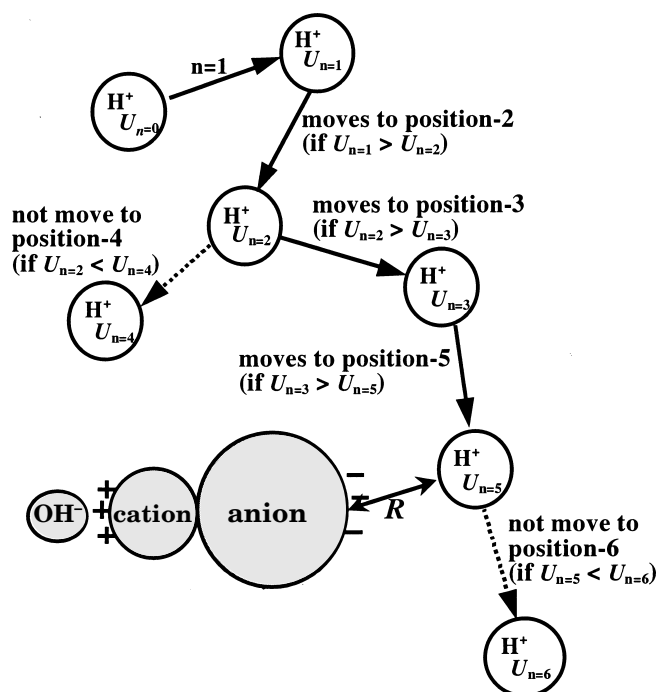
Figure 6. Diagram of simulation of ion retransferring to negative CCA-OH. At each movable step, H+ moves to the next step according to Boltzmann distribution, at 300K. R is obtained in the simulation. Finally, a ten thousand number of R is obtained for one CCA through 100,000 simulations.

Counting Number of H+ Around CCA-OH. The decrease in the CCA toner charge magnitude was simulated by counting the number of H+ ions attracted to CCA-OH, using a new program developed by us in which the Monte Carlo method (MC) and the energy minimization method were combined. We explain our computational process as follows and illustrate it in Fig. 6. The first step is the determination of the initial coordinates of H+ around CCA–OH at a distance of 5nm away, using MC. This operation is described as $n = 0$, n meaning the number of iterations in the MC process, that is to say, the number of steps of moving H+ ion around CCA–OH. In the second step ($n = 1$), the H+ is moved in a restricted direction and distance according to the random number in MC, and the coordinate is determined. The potential energy between CCA–OH and H+ is then calculated. The potential energy ($U_{n=1}$) includes the Van der Waals potential ($U_{v,\ n=1}$) and the coulomb potential ($U_{c,\ n=1}$) as in Eq. 1. The Van der Waals potential is expressed by Eq. 2[17] and the coulomb potential by Eq. 3.

$$U = U_v + U_c \tag{1}$$

$$U_v = Ar^{-12} - Br^{-6} \tag{2}$$

$$U_c = \frac{q_m q_n}{4\pi\varepsilon_0 d_{mn}} \tag{3}$$

wherein the symbols have their usual meanings.

In the third step ($n = 2$), the new H+ coordinate is determined and the potential energy ($U_{n=2}$) at the new position of CCA-OH and H+ is calculated, using the same methods as in the foregoing step. If the $U_{n=2}$ is less than $U_{n=1}$, H+ moves to the new coordinate ($n = 2$) with the probability $P = e^{-\Delta U/RT}$ according to the Boltzmann distribution at $T = 300$K. However if the $U_{n=1}$ is less than or equal to $U_{n=2}$, H+ does move but stays at the $n = 1$ position. These operations are repeated up to the set number in the program; thereby H+ is able to move along a stable path. All the while the atomic charges don't change. We emphasize the use of the Boltzmann distribution. In general, the condition for use of the distribution requires that a temperature is not extremely low, and that the number of available states is considerably greater than the number of existant molecules. Therefore, the motion of H+ ions near CCA–OH and with energy approximately equivalent to the minimum is under control of the essential properties of H+ ions rather than under that of the Boltzmann distribution, because the number of available states of H+ near CCA–OH is less than exist far away from it. Hence, when H+ approaches close to the CCA–OH, within 0.3 nm in our calculations. We disengage the motion of H+ from the limitation of the Boltzmann distribution and make the motion depend on only the energy difference of the two compared positions. The motion is illustrated in Fig. 6 according to the above calculation. Thus we obtained the minimum distance of H+ from CCA–OH, R(nm), in one operation. The operation was repeated 100,000 times for one CCA. Finally, we obtained the number distribution of H+ versus each R.

Six complicated compounds were prepared as negative CCA. They were organic metal complexes in three categories based on ligand. Each ligand was dibutyl salicylic acid or salicylic acid, or a naphthoic acid derivative, and had a large and complex molecular structure. Each complicated chemical structure is indicated in Fig. 7. Bis[3-hydroxy-2-naphthoate(o,o')(2-)] diaquachrom(III) acid Hydrogen salt (CCA–**A**), bis[3,5-di-tert-butyl-2-hydroxybenzoate(o,o')(2-)]zinc(II) acid 2 Hydrogen salt (CCA–**B**), tris-[3,5-di-tert-butyl-2-hydroxybenzoate(o,o')(2-)] aluminium(III) (CCA-**C**), and bis-[1-(2-hydroxy-3,5-dinitrophenylazo)-3-phenyl carbamoyl-2-naphtho-late(o,o')(2-)] chrom(III) acid Hydrogen salt (CCA–**D**) can be commercially obtained. Bis-[3,5-di-tert-butyl-2-hydroxybenzoate(o,o')(2-)] boron(III) acid potassium salt (CCA–**E**) and bis-[2-hydroxybenzoate(o,o')(2-)] boron(III) acid potassium salt (CCA–**F**) were synthesized by us in trial production. The chemical structures except for CCA–**C**, are composed of a large anion and a small cation. The CCA–**C** chemical structure is not a salt type that comprises of an anion and a cation, rather a large coordination complex. It is indispensable to verifying the IRM, because its ability to decrease the negative CCA charge by attracting H+ is expected to be weak, because a large anion or molecule as this CCA has a weak negative charge distribution on its surface. Additionally, the cation must concentrate positive charges on its surface in order to verify the ion retransfer model, because the charge convergence is needed for a CCA toner which is negatively charged due to the dissociation of water molecules and the attraction of the OH- ions.

We next prepared the CCA toner for measuring the triboelectric charge magnitude. The CCA existed only on the toner particle surface. The reason for preparing the external CCA toner was to reduce the influence of many factors on toner charging phenomenon other than the CCA molecule, based on the presupposition in the section, Charging Model. The toner was a mixture of 9.04×10^{-4} mol CCA and 40g of styrene-acrylic copolymer particles with an average diameter approximately of 12 μm, made using a high speed fluid mixer at 13000
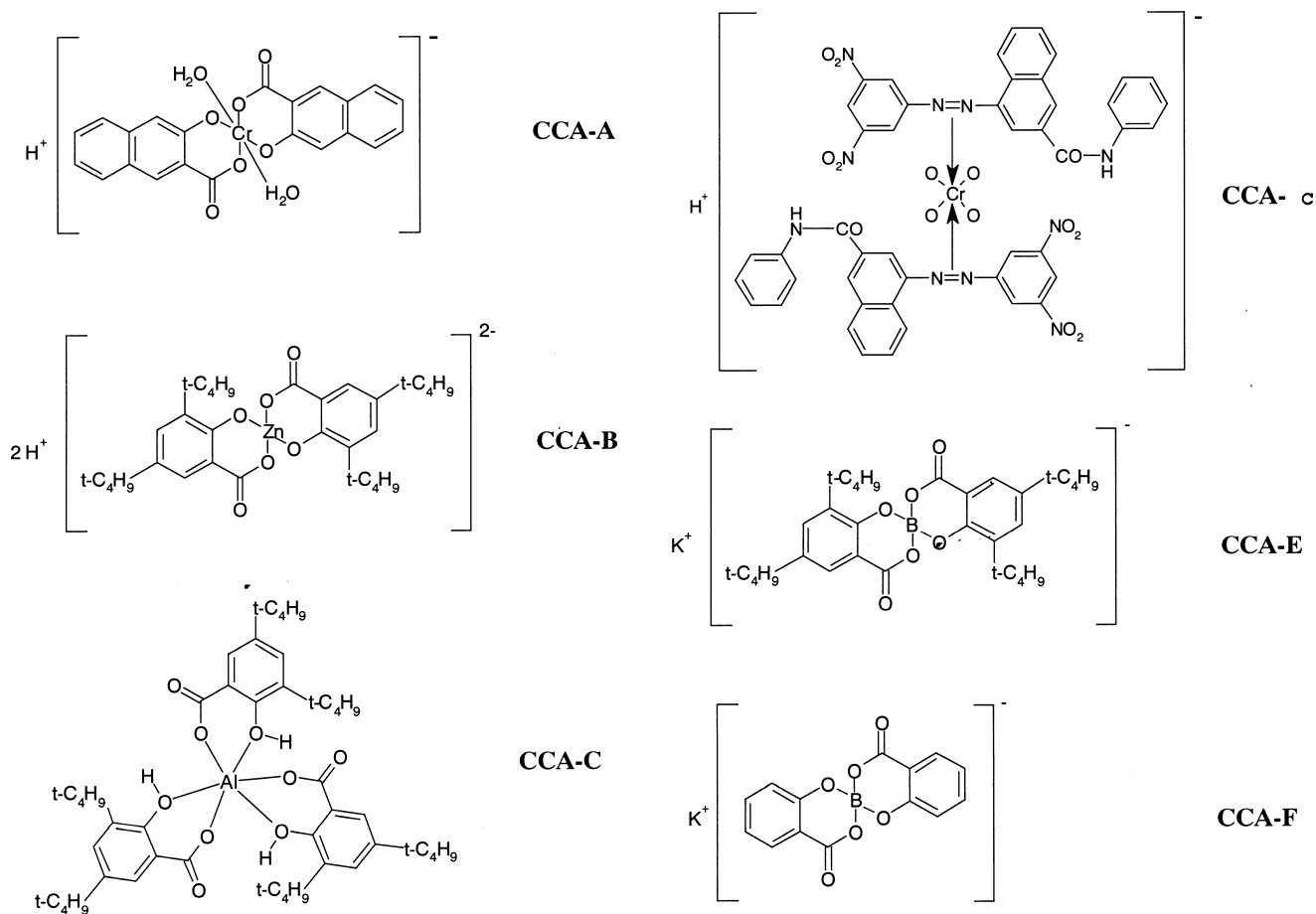
Figure 7. Molecular structure of negative CCA.

rpm for 30 s. This method is the same as that for testing the WDM. We have already obtained excellent results thereby in the previous study.[14,15]

In the measurement of the triboelectrification charge for the CCA toner, 100 μm steel shot was used as the carrier. A mixture of 3 wt% toner and 97 wt% carrier was prepared and mixed with a high speed mixer. Sampling was carried out after mixing for 5, 10, 20, 30, 60, 180 s; 5, 10, 15, 20, 25, 30, 40, 50, 60, 80, 100, 120, 150 min; and at intervals of 30 min until obtaining the maximum triboelectrification charge (q_m) was obtained. The triboelectrification charge were measured with a blow-off method, in which the charge of the carrier remaining in a steel cage was measured after blowing off the toner with dry nitrogen gas jet. The polarity of toner's charge is contrary to the measured charge. The q_m is regarded as the representative triboelectrification charge for the CCA toner, because its magnitude results from charging due to the attraction of water ions of the same polarity as the CCA charging, decreased or increased due to retransferred water ions.

Results

In every case, most of the hundred thousand or so associated H+ ions exist far from the virtual complex, the CCA-OH, the remaining ions are small in number and exist near the complex, resulting from calculations based on the IRM. The distribution by number of H+ ions over dis-
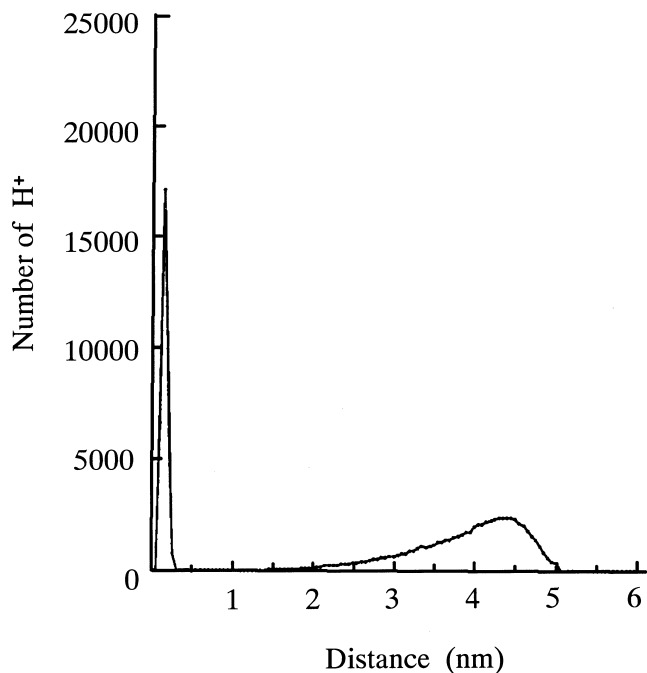

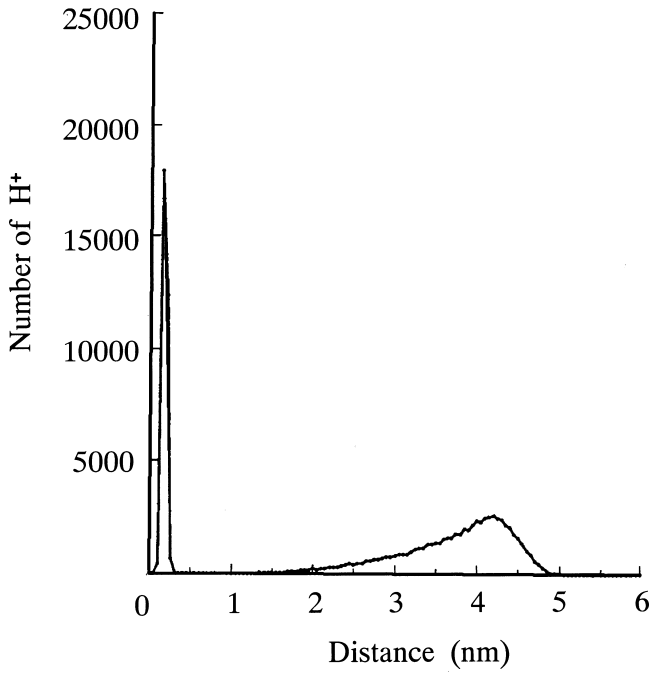**Figure 8**. The distribution by number of H+ near CCA-**A**-OH, after 100,000 trials.

Figure 9. The distribution by number of H+ near CCA-**B**-OH, after 100,000 trials.
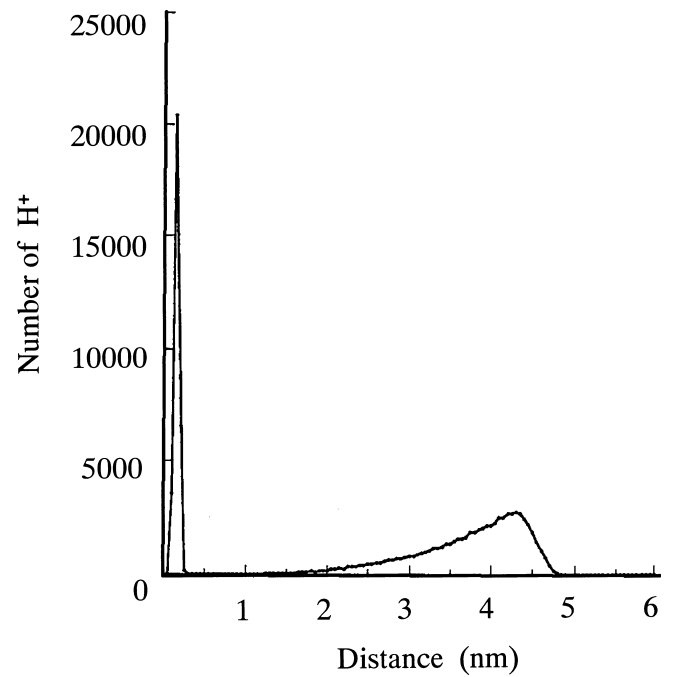

Figure 11. The distribution by number of H+ near CCA-**D**-OH, after 100000 trials.
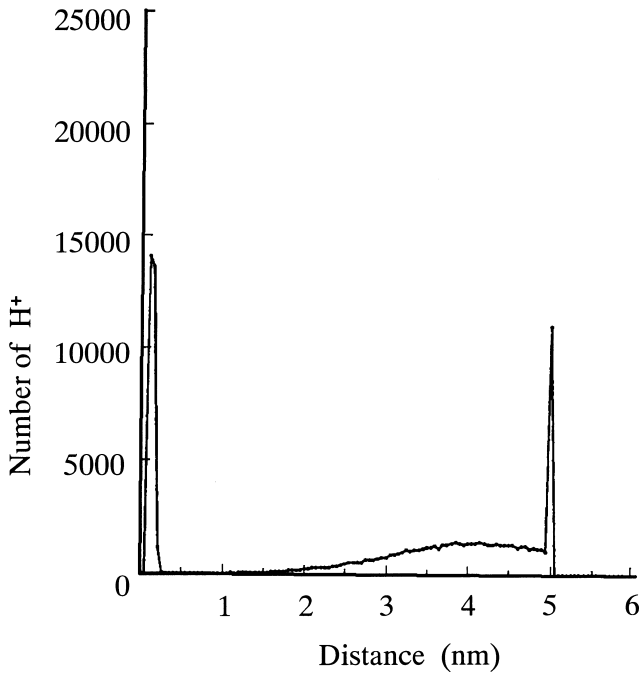

Figure 10. The distribution by number of H+ near CCA-**C**-OH, after 100000 trials.
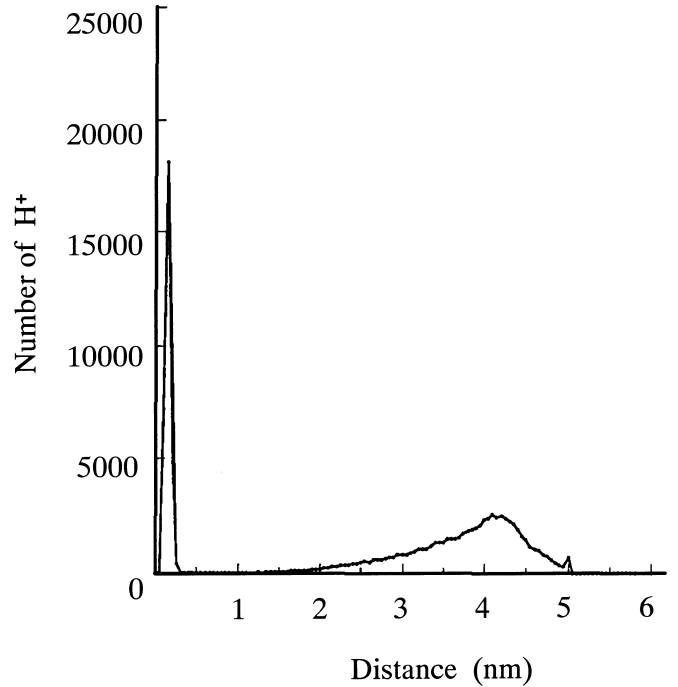

Figure 12. The distribution by number of H+ near CCA-**E**-OH, after 100000 trials.

tance from the CCA–OH typically shows a bimodal form as in Fig. 8 through Fig. 13. About 30% of all H+ exists within 0.4 nm from CCA–OH, and the residual 70% H+ is scattered widely over the range of 1 ~ 5 nm (Table I). The former small fraction is regarded as ions retransferring from the carrier bead surface and causes the CCA charge decrease; we noted in particular the number of H+ ions in the range of $0.1 \leq R < 0.15$ nm, because R is then of sufficient magnitude for H+ to interact with CCA–OH. The number for CCA–**C** is the largest and is 14092; it is

7307 on CCA–**F**, 7194 on CCA–**E**, 6613 on CCA–**A**, and 396 on CCA–**B**, in decreasing order.

All maximum triboelectric charges (q_m) observed are listed in the lowest row of Table I. It is lowest in the case of CCA–**C**, -10.2 μc/g. The charge increases in the order of CCA–**C**, CCA–**A** ≈ CCA–**E** ≈ CCA–**F**, CCA–**B** ≈ CCA–**D** taking into consideration experimental error. A comparison of both orders shows a definite correlation between the calculated number based on the IRM and the observed maximum triboelectric charge. We show this correlation
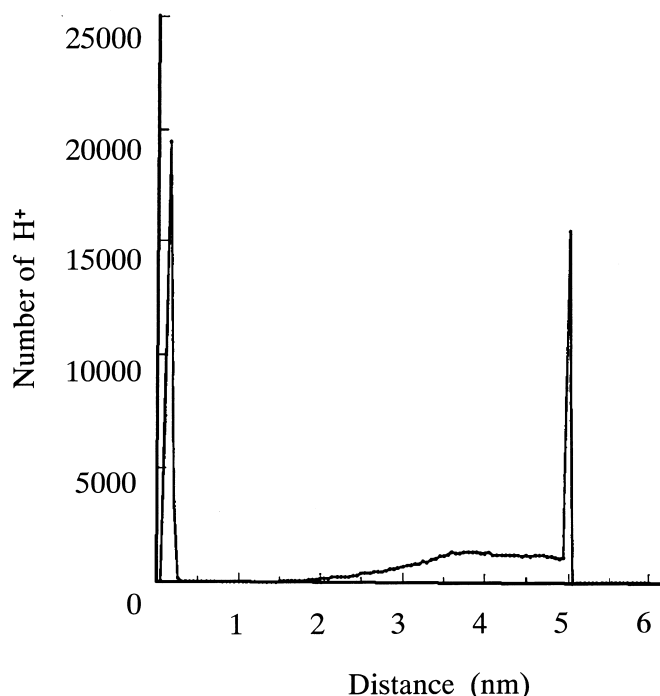
Figure 13. The distribution by number of H+ ions near CCA-F-OH, after 100,000 trials.
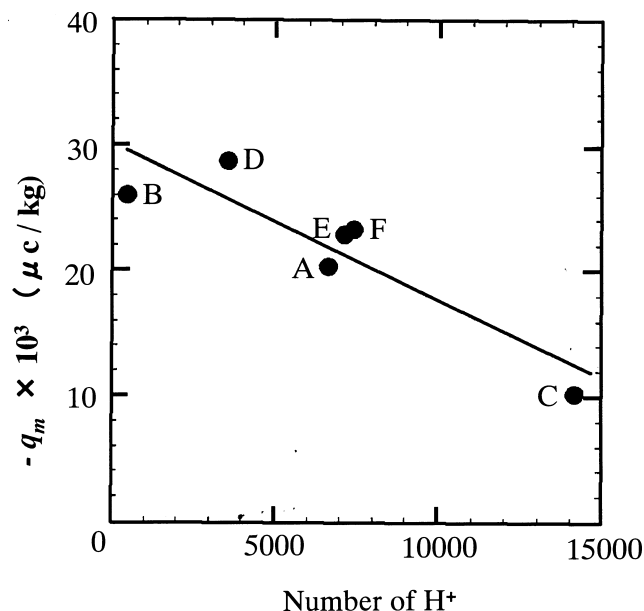

Figure 14. Correlation between number of H+ ions and maximum triboelectric charge. The number shows it of the H+ exists near by the CCA-OH in the range of $0.1 \leq R < 0.15$ nm, after 100,000 trials.

TABLE I. The Number of H+ Ions Approaching CCA–OH

R (nm)/CCA	A	B	C	D	E	F
$0 < R < 0.05$	0	0	0	0	0	0
$0.05 \leq R < 0.1$	0	0	0	0	0	0
$0.1 \leq R < 0.15$	6613	396	14092	3549	7194	7307
$0.15 \leq R < 0.2$	17115	17924	13601	20387	18112	19420
$0.2 \leq R < 0.25$	6267	l2380	1146	6528	4842	3545
$0.25 \leq R < 0.3$	770	645	47	203	380	200
$0.3 \leq R < 0.35$	3	1	0	3	4	3
$0.35 \leq R < 0.4$	0	0	0	0	1	0
subtotal	30768	31346	28886	30670	30533	30475
$0.4 \leq R < 5.0$	69232	68654	71114	69330	69467	69525
total	100000	100000	100000	100000	100000	100000
$q_m \times 10^{-1}$ (μC/kg)	−15.2	−18.0	−10.2	−19.4	−16.5	−16.6

Calculating conditions: Trail times—100,000; Maximum steps of n—1.000; Temperature—300K; Emergence radius of H+ from CCA-OH—5 nm; Criterion of termination—continuous staying at same position during 30 steps.

in Fig. 14. We found that as the number of H+ in the range increases, the greater was the decrease in the CCA toner's triboelectric charge, q_m, in Fig. 14. This tendency is consistent with the prediction from the IRM.

Discussion

It is necessary for the results to confirm that the negative CCA molecule possesses the same ability for dissociating water molecules and the same ability for attracting OH− ions. Both the abilities are regarded as an index of negative charging in WDM. The model, IRM, for the negative CCA should permit predicting that the change in the CCA charging magnitude depending on the difference in the steric structure and the charge distribution in the region with dispersed negative charges, but only if the region with concentrated positive charges of the CCA molecule possesses comparable abilities. To confirm this uniformity, we calculated the charge on each atom of a water molecule influenced by the CCA for all CCA. The results, which are is listed in Table II, indicate that there is no great difference in the absolute charge on one oxygen atom or on two hydrogen atoms among the CCA. Consequently, we regard the ability for charging negatively of all CCA as the same.

The calculated and observed results agree approximately with prediction from the IRM. The CCA, which attracts more H+, reduces the negative charge magnitude in Fig. 14. In addition to this result, each point falls neatly on a line, though every CCA possessed a complicated and varied chemical structure. This result supports the assumption based on the IRM. Furthermore, the result is remarkable because no coherent result has been obtained on the correlation between the calculated charge magnitude and that observed for various materials used in electrophotography. In the former

TABLE II. Calculated Charge on the Atoms Composing a Water Molecule Under CCA's Influence

CCA	Type of Molecular Structure	Net Charge x 10^{19}(C)		
		0	H(1)	H(2)
A	Salt	-1.09	0.54	0.54
B	salt	-1.09	0.54	0.54
C	non-salt	-1.17	0.59	0.59
D	salt	-1.08	0.54	0.54
E	salt	-1.10	0.55	0.55
F	salt	-1.10	0.55	0.55

H(1) nearly exists CCA molecule more than H(2)

study various mechanisms have been proposed according to the respective molecular structures. There was no systematic mechanism to explain the influence of the molecular structure of CCA on CCA charging, and the mechanism applied to only a restricted series of compounds. Hence in the past molecular design for a superior CCA depended empirically on the analogy of chemical structure described on paper, using classical parameters, i.e., electronegativity. Consequently, it often happened that the toner containing a given compound as the CCA did not charge according to expectations. However if a simulation based upon the WDM and the IRM is used, a highly accurate molecular design should be possible.

Conclusions

The IRM is proposed as one charging mechanism that can be used to interpret the correlation between the molecular structure of CCA and its triboelectric charging property. The model is complimentary to WDM and is characterized by observing the water molecule's involvement in the CCA charging phenomenon. It interprets the CCA charging ability in terms of the ability to attract an ion counter to the CCA charge polarity, i.e., OH^- or H^+ dissociated from a water molecule. The model is verified by comparing the results from calculations based on the model with those observed with various CCA having a complicated chemical structure for which the charging properties could not be predicted. The calculated number of H^+ ions close to the CCA molecule

was found to depend on this complicated molecular structure and charge distribution. Additionally the increase in the number was found to be consistent with the decrease in the observed triboelectric maximum charge magnitude. This result supports the model and suggests the possibility of predicting the charge property through a theoretical calculation based only on molecular structure. ⚠

References

1. J. H. Anderson and D. E. Bugner, *Proceedings of The 4th International Congress on Non-Impact Printing Technologies*, IS&T, Springfield, VA, 1988, p. 79.
2. H. W. Gibson, *Polymer Science and Technologies* **21**, 353 (1983).
3. T. Nanya and K. Tsubuko, *Proceedings of The 30th Anniversary Conference of The Society of Electrophotography of Japan*, Tokyo, JP, 1988, p. 9.
4. K. Hashimoto, H. Akagi, H. Matsuoka, and H. Soyama, *Proceedings of The Annual Conference of Japan Hardcopy for the Society of Electrophotography of Japan*, Tokyo, JP, 1990, p. 9.
5. O. Okada and K. Oka, *J. Soc. Electrophotography of Japan* **30,** 445 (1991).
6. H. A. Mizes, E. M. Conwell, and D. P. Salamida, *Appl. Phys. Lett.* **56**, 1597 (1990).
7. M. Anzai and H. Yamaga, *Proceedings of the Joint Seminar of The Society of Electrophotography of Japan and of The Institute of Electrostatics Japan*, Tokyo, JP, 1990, p. 35.
8. T. Oguchi and M. Tamaya, *Oyo Butsuri* **52**, 674 (1983).
9. L. B. Schein, *J. Imaging Sci. Technol.* **37**, 1 (1993).
10. A. Kondo, *Proceedings of the 43rd Sympo. of the Soc. of Electrophotography of Japan*, Tokyo, JP, 1979, p. 26.
11. R. Kurita, *J. Soc. of Electrophotography of Japan* **26**, 126 (1987).
12. L. H. Lee, *Photogra. Sci. Eng.* **22**, 228 (1978).
13. J. H. Anderson, *J. Imaging Sci. Technol.* **38**, 378 (1994).
14. N. Matsui, K. Oka, and Y. Inaba, *Proceedings of The 6th International Congress on Advances in Non-Impact Printing Technologies*, Tokyo, JP, 1990, p. 123.
15. N. Matsui, Oka, K., and Y. Inaba, *J. Soc. of Electrophotography of Japan* **30**, 282 (1991).
16. N. Matsui and K. Oka, *Proceedings of The 61st Spring Congress of the Chem. Soc. of Japan,* Tokyo, JP, 1992, p. 996.
17. S. L. Mayo, B. D. Olafson, and W. A. Goddard III, *J. Phys. Chem.* **94**, 8897 (1990).
18. A. K. Rappe and W. A. Goddard III, *J. Phys. Chem.* **9**, 3358 (1991).
19. M. J. Dewar and S. W. Thiel, *J. Am. Chem. Soc.* **99**, 4899 (1977).